

**Experimental and Theoretical Studies  
of the LiBH<sub>4</sub>-LiI Phase Diagram**

**Asya Mazzucco,<sup>a)</sup> Erika Michela Dematteis,<sup>a)</sup> Valerio Gulino,<sup>a)b),§</sup> Marta Corno,<sup>a)</sup> Mauro Francesco Sgroi,<sup>a)</sup> Mauro Palumbo,<sup>a)</sup> Marcello Baricco<sup>a)</sup>**

a) Department of Chemistry, Inter-departmental Center NIS and INSTM, University of Turin, Via Pietro Giuria 7, 10125 Torino, Italy

b) Materials Chemistry and Catalysis, Debye Institute for Nanomaterials Science, Utrecht University, Universiteitsweg 99, 3584 CG, Utrecht, The Netherlands

§ Present address: LeydenJar, Luchthavenweg 10, 5657 EB Eindhoven, The Netherlands

**Supplementary Information**

### XRD and Rietveld analysis of as-prepared samples

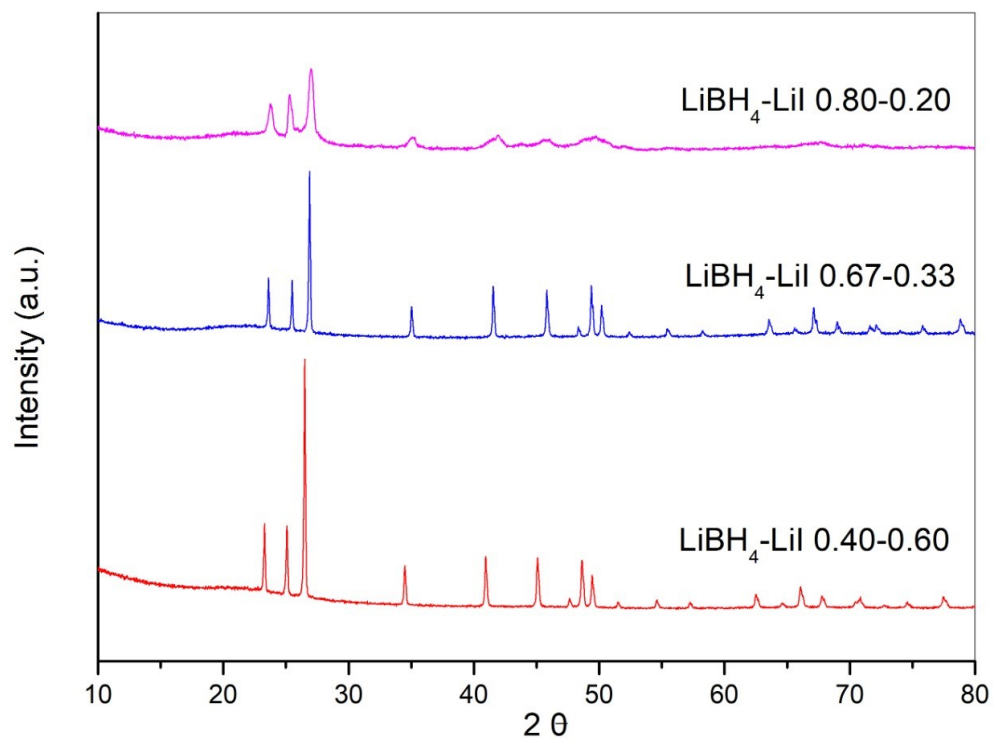


**Figure S1** XRD pattern of sample S2 (bottom), S4(middle) and S5 (top).

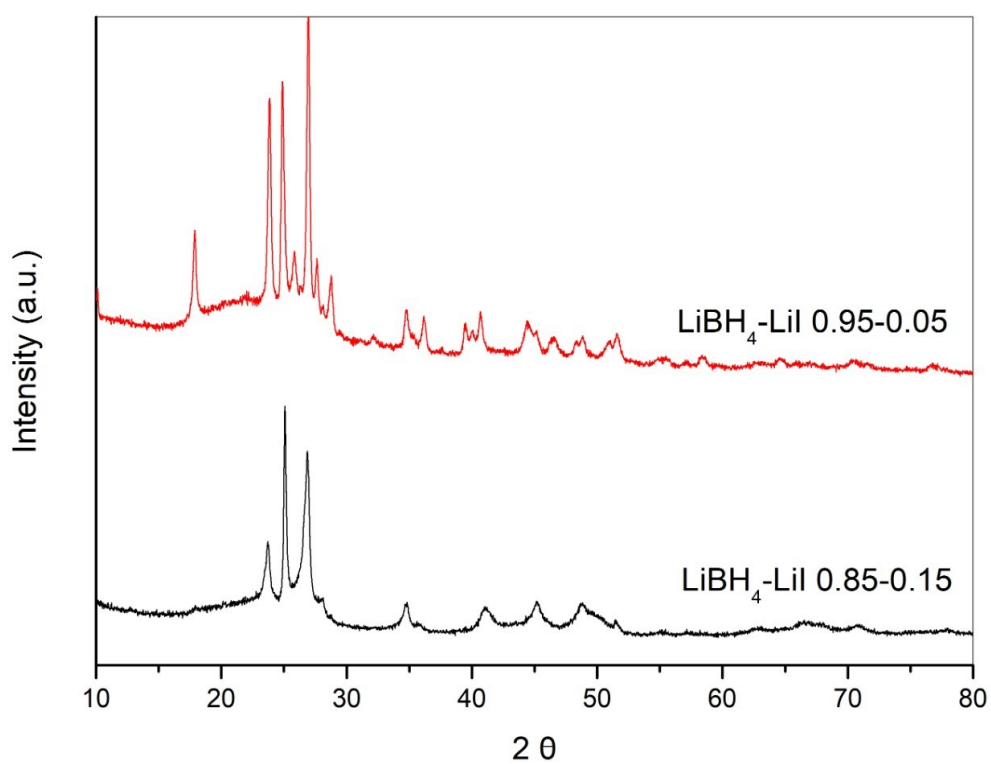


**Figure S2** XRD pattern of sample S6 (bottom) and S8 (top).

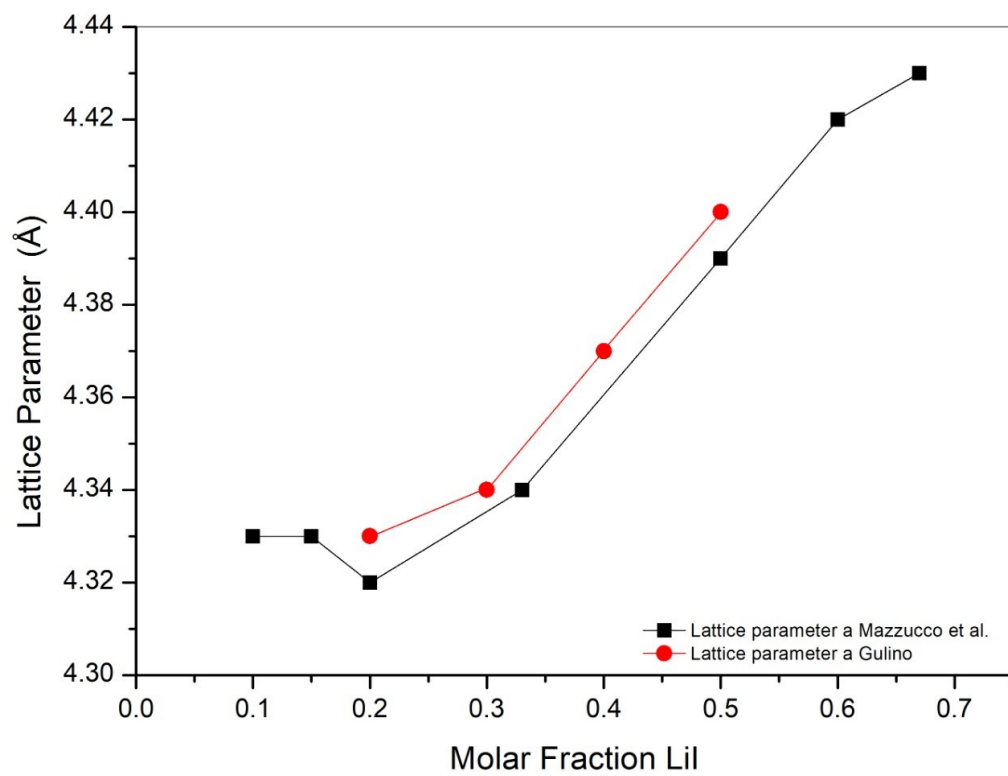


**Figure S3** Comparison of the lattice parameter  $a$  of the hexagonal phase. Connecting lines are a guide for the eyes. Lattice parameters have been obtained in this work (black squares) and in ref.[1] (red circles).

Fare clic o toccare qui per immettere il testo.

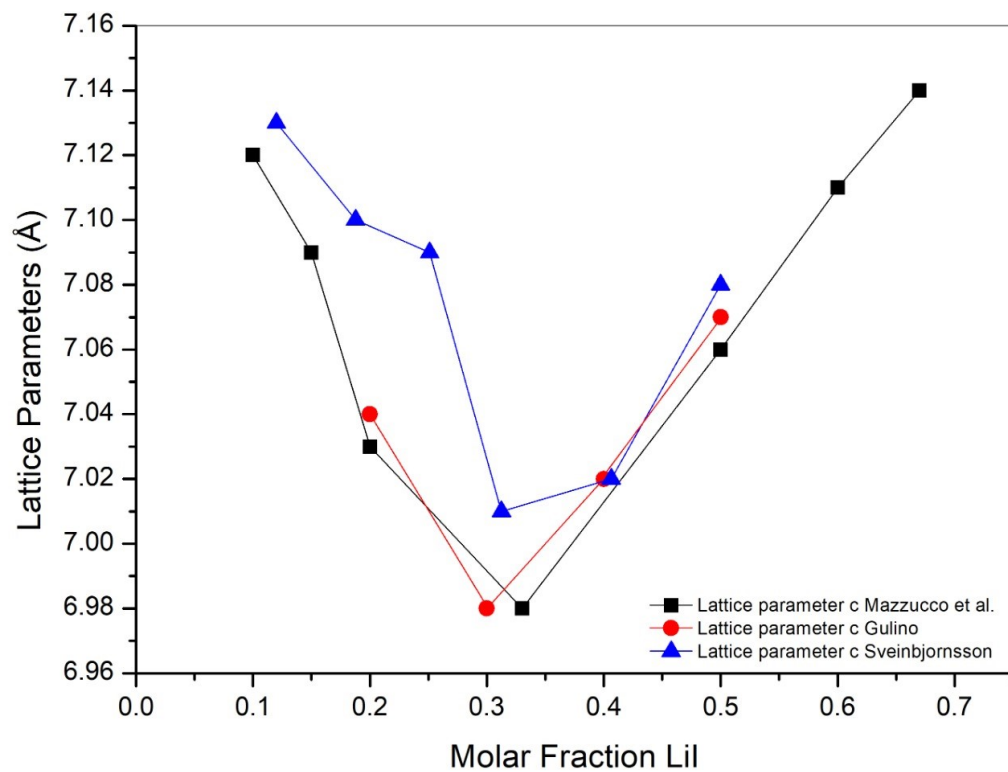


**Figure S4** Comparison of the lattice parameter  $c$  of the hexagonal phase. Connecting lines are a guide for the eyes. Lattice parameters have been obtained in this work (black squares), ref.[1] (red circles) and ref.[2] (blue triangles).

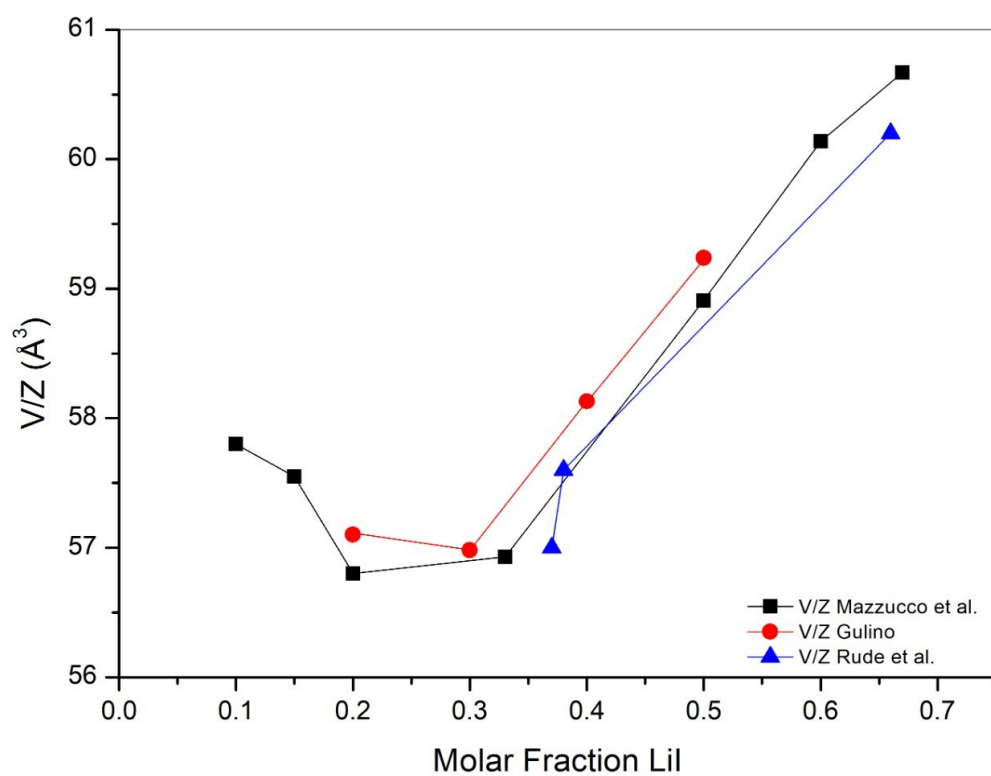


**Figure S5** Comparison of  $V/Z$  of the hexagonal phase. Connecting lines are a guide for the eyes.  $V/Z$  values have been obtained in this work (black squares), in ref.[1] (red circles) and in ref.[3] (blue triangles).

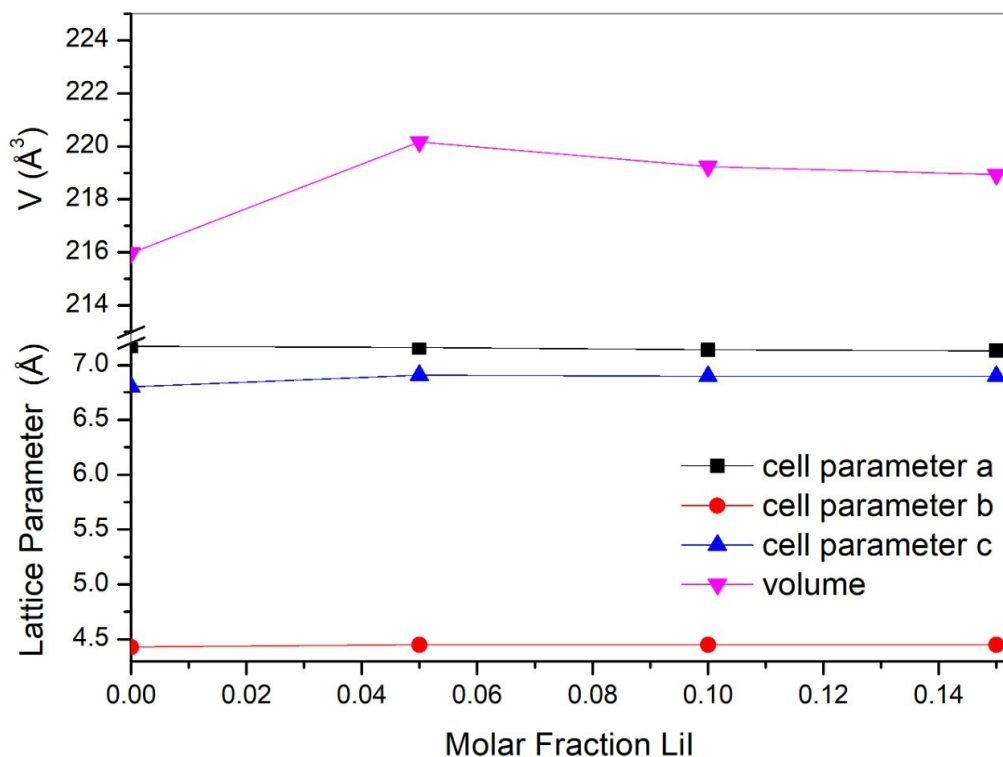


**Figure S6** Lattice parameters *a*, *b*, *c* and volume of orthorhombic phase of samples S6, S7 and S8. Connecting lines are a guide for the eyes.

Sample - Molar fraction LiI	LiBH <sub>4</sub> Hexagonal from Rietveld (% mol)	Lever rule (% mol)
S7-0.10	38	38
S6-0.15	76	77

**Table S1** Comparison of LiBH<sub>4</sub> hexagonal phase %mol by Rietveld Refinement and lever rule

Sample - Molar fraction LiI	Occupancy
S7-0.10	0.183
S6-0.15	0.179
S5-0.20	0.225
S4-0.33	0.365
S3-0.50	0.515
S2-0.60	0.604
S1-0.67	0.604

**Table S2** Occupancy of the 2b site in the hexagonal structure obtained by the Rietveld refinement.

Sample	Orthorombic Phase Cell parameters			Hexagonal Phase Cell parameters		Cubic Phase Cell parameter
	a	b	c	a	c	a
LiI pure	/	/	/	/	/	6.03
S1	/	/	/	4.43	7.14	6.03
S2	/	/	/	4.42	7.11	/
S3	/	/	/	4.39	7.06	/
S4	/	/	/	4.34	6.98	/
S5	/	/	/	4.32	7.03	/
S6	7.13	4.45	6.9	4.33	7.09	/
S7	7.14	4.45	6.9	4.33	7.12	/
S8	7.16	4.45	6.9	/	/	/
LiBH <sub>4</sub> pure	7.17	4.43	6.8	/	/	/

**Table S3** Cell parameters of various crystal structures of all the prepared samples. Values are reported in Å.

### IR-ATR analysis

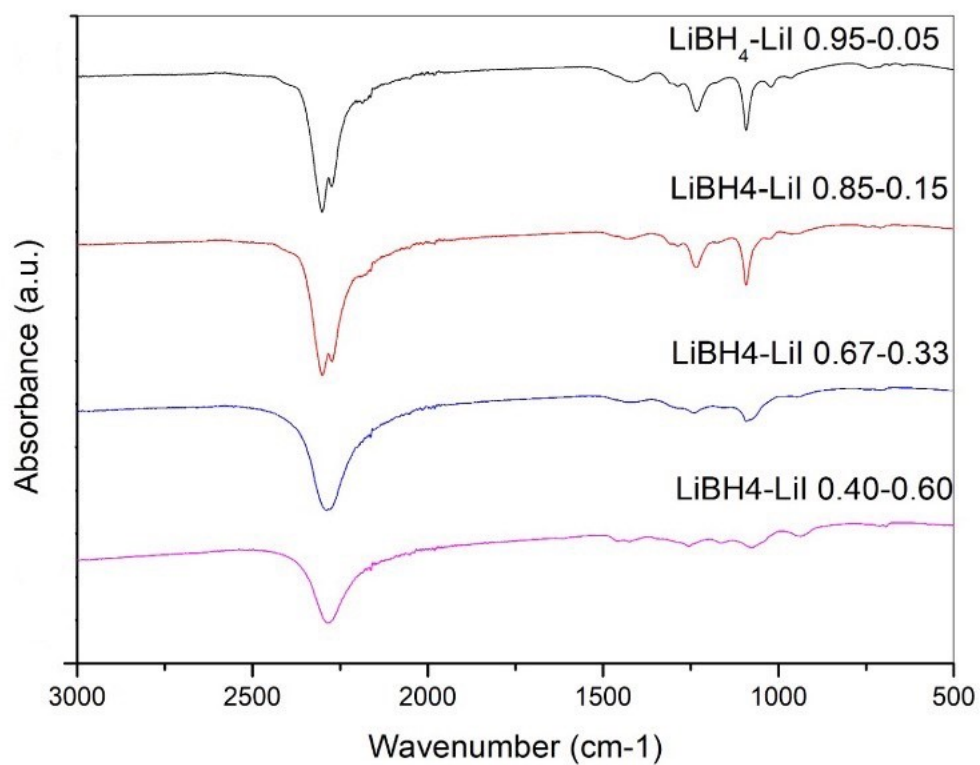


**Figure S7** IR-ATR spectra of sample (starting from the bottom): S2 (first), S4(second), S6 (third) and S8 (last).



DSC analysis

$\text{LiBH}_4\text{-LiI } 0.33\text{-}67$

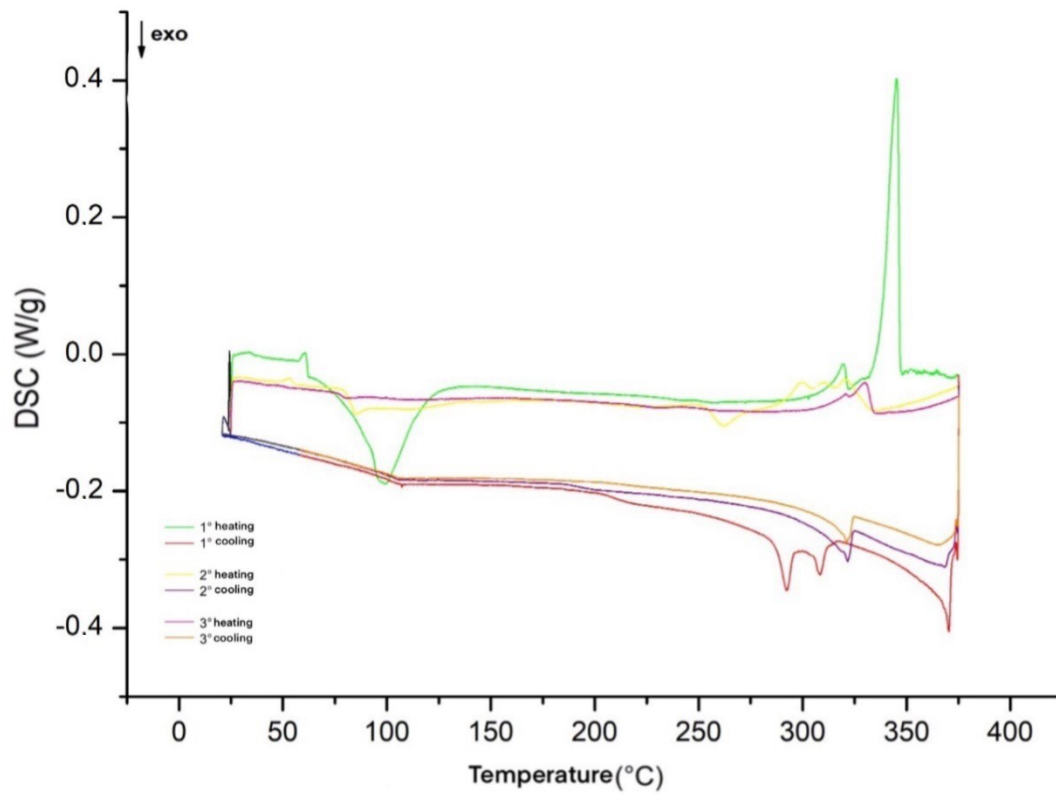


Figure S8 DSC trace of sample S1.

$\text{LiBH}_4\text{-LiI } 0.40\text{-}0.60$

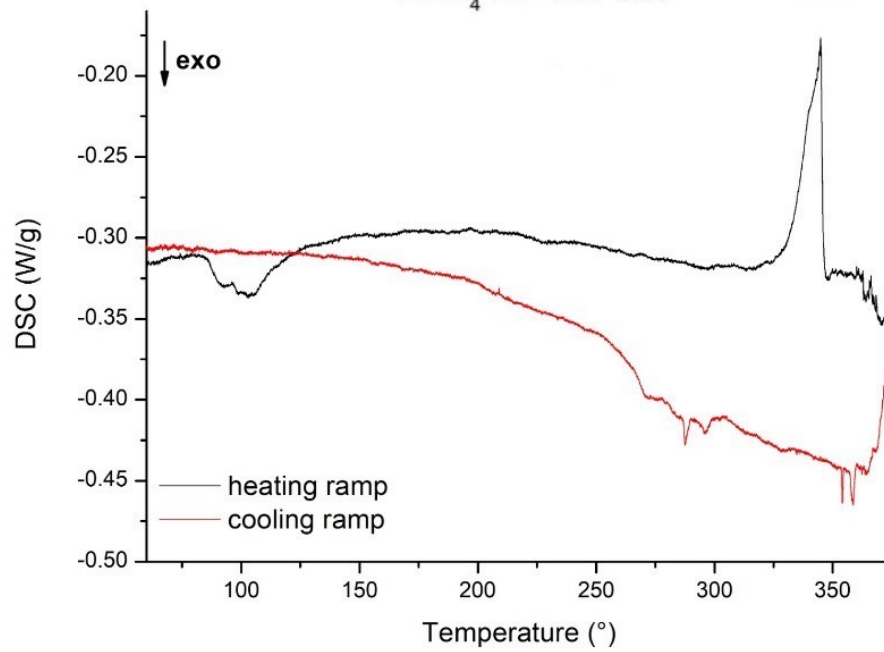
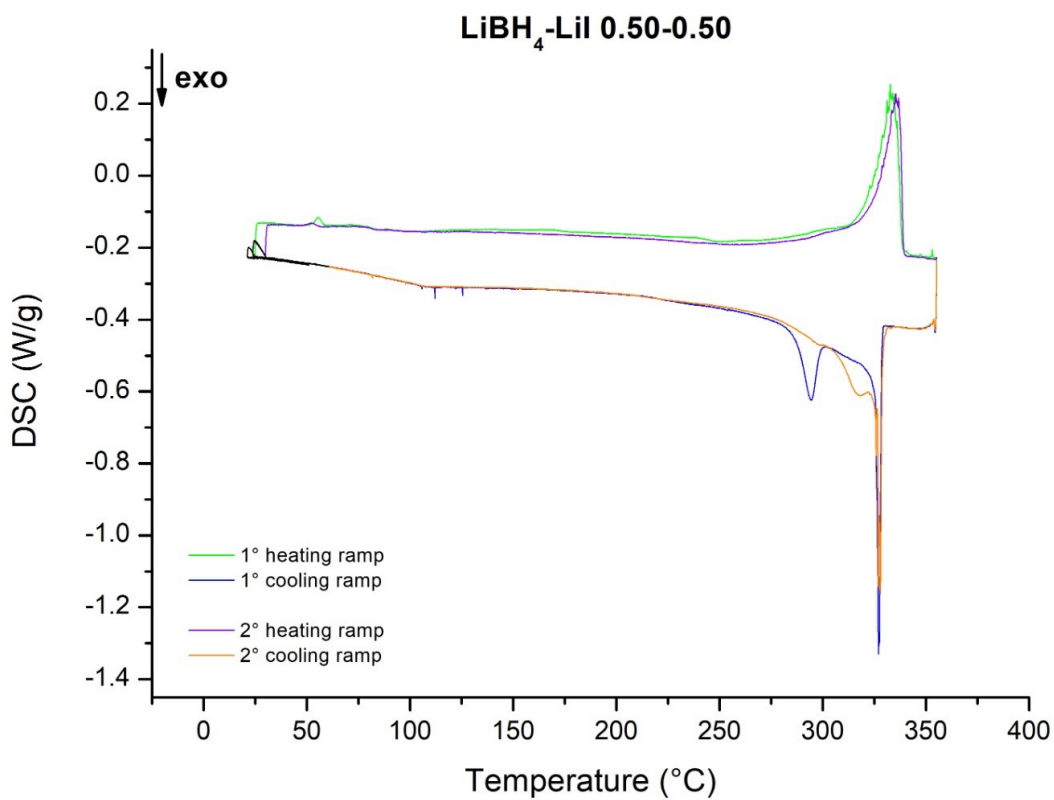
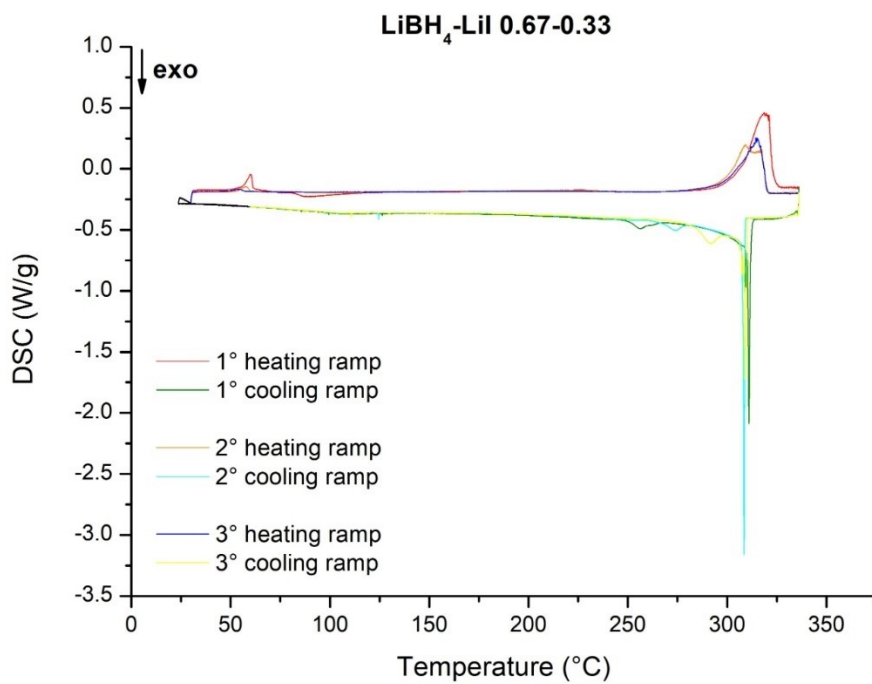


Figure S9 DSC trace of sample S2.



*Figure S10* DSC trace of sample S3



*Figure S11* DSC trace of sample S4.

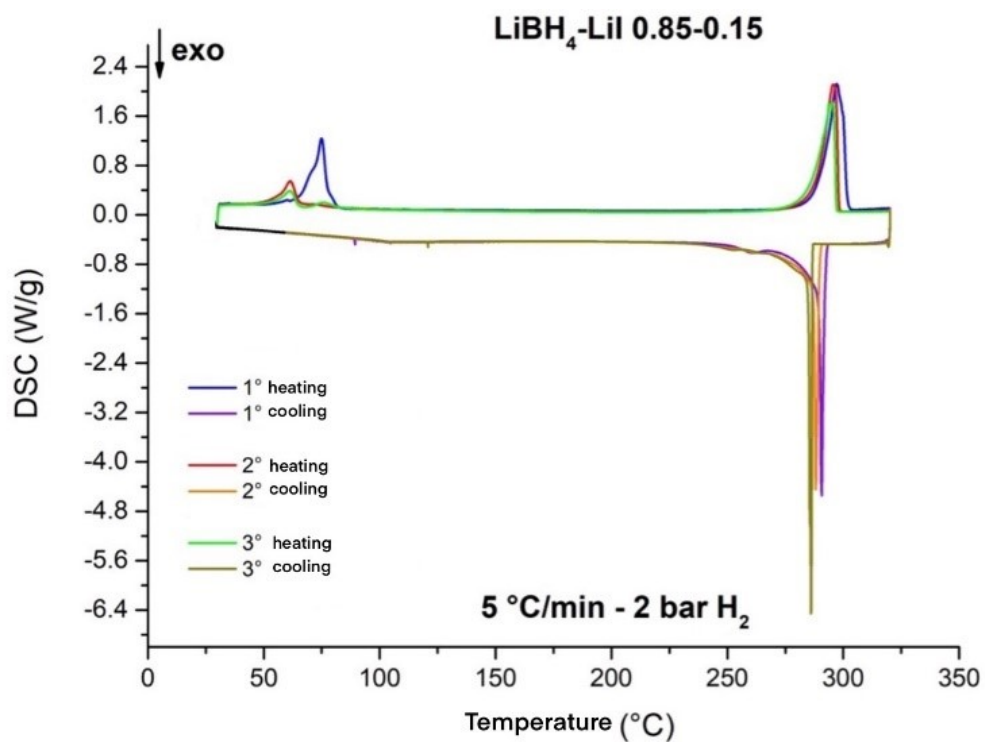


Figure S12 DSC trace of samples S6.

x

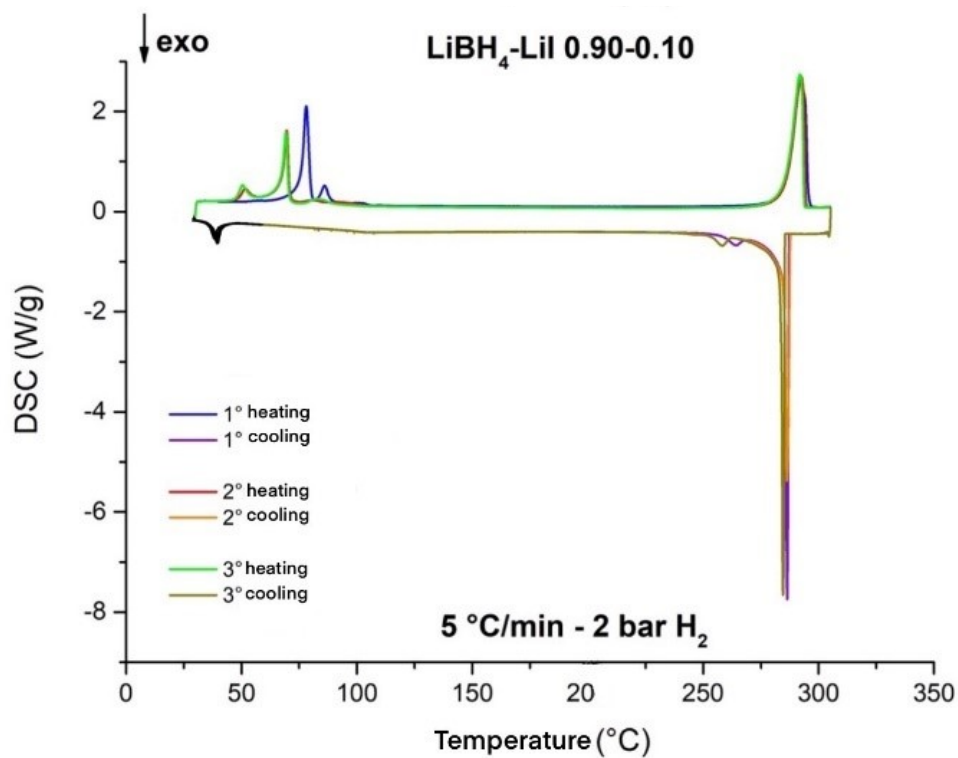
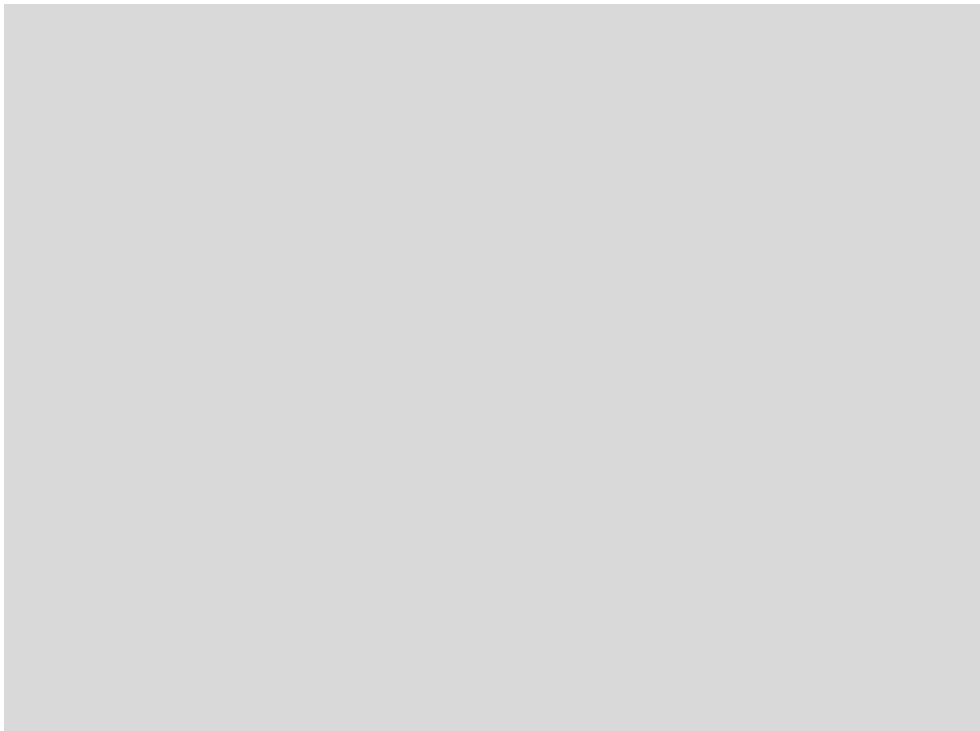
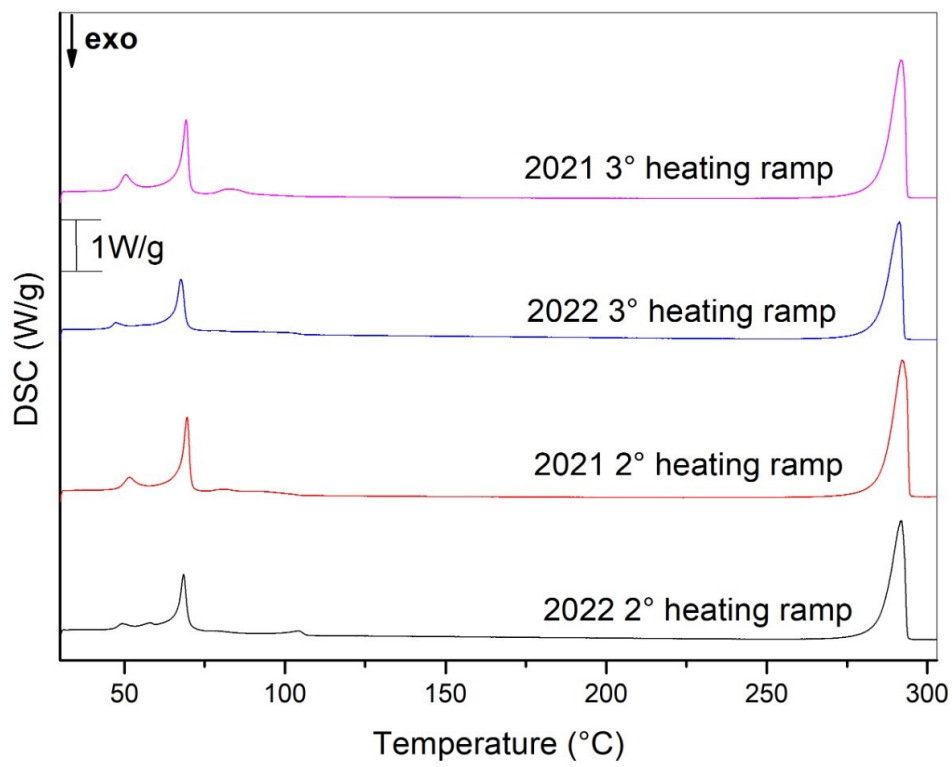


Figure S13 DSC trace of sample S7.



**Figure S14** DSC trace of sample S8.



**Figure S15** DSC trace of sample S7 - 2021 vs 2022 measurements.

Sample S1	Temperature	Enthalpy
LiBH <sub>4</sub> -LiI 0.33-0.67	°C	kJ/mol
Peritectic	294	0.2
Melting	329	1.9

*Table S4* Peritectic point and melting temperatures, with corresponding enthalpies, of sample S1.

Sample S2	Temperature	Enthalpy
LiBH <sub>4</sub> -LiI 0.40-0.60	°C	kJ/mol
Melting	317	1.4

*Table S5* Melting temperature and corresponding enthalpy of sample S2.

Sample S3	Temperature	Enthalpy
LiBH <sub>4</sub> -LiI 0.5-0.5	°C	kJ/mol
Melting	307	7.2
Solidification peak 1	333	-4.1
Solidification peak 2	303	-2.8

*Table S6* Melting and solidification temperatures, with corresponding enthalpies, of sample S3.

Sample S4	Temperature	Enthalpy
LiBH <sub>4</sub> -LiI 0.67-0.33	°C	kJ/mol
Transition	50	0.4
Melting	288	5.5
Solidification peak 1	315	-4.1
Solidification peak 2	270	-1.2

*Table S7* Transition, Melting and Solidification temperatures, with corresponding enthalpies, of sample S4.

Sample S6	Temperature	Enthalpy
LiBH <sub>4</sub> -LiI 0.85-0.15	°C	kJ/mol
Transition	60	4.2
Melting	285	8.3
Solidification	293	-7.5

*Table S8* Transition, Melting and Solidification temperatures, with corresponding enthalpies, of sample S6.

Sample S7	Temperature	Enthalpy
LiBH <sub>4</sub> -LiI 0.90-0.10	°C	kJ/mol
Transition peak 1	66	3.3
Transition peak 2	81	0.9
Melting	284	7.7
Solidification	287	-6.7

*Table S9* Transition, Melting and Solidification temperatures, with corresponding enthalpies, of sample S7.

<b>Campione S8</b>	<b>Temperature</b>	<b>Enthalpy</b>
<b>LiBH4-LiI 0.95-0.05</b>	<b>°C</b>	<b>kJ/mol</b>
<b>Transition peak 1</b>	73	3.9
<b>Transition peak 2</b>	91	0.4
<b>Melting</b>	280	5.9
<b>Solidification</b>	284	-5.9

*Table S10* Transition, melting and solidification temperatures, with corresponding enthalpies, for sample S8.

### Enthalpy of Mixing

In order to obtain the value of the enthalpy of mixing, the real composition of the hand mixed sample was taken in consideration by using the enthalpy of transition of pure  $\text{LiBH}_4$ , acquired by the integration of the endothermic peak at  $111\text{ }^\circ\text{C}$  of the DSC trace (Figure ), as an internal standard by fixing the value at  $241.48\text{ J/g}$  (i.e.  $5.3\text{ kJ/mol}$ ). By using this approach, the  $\text{LiI}$  molar fraction of each sample was obtained. Therefore, the obtained molar composition was used for the calculation of the enthalpy of mixing.

The integration peak used for the enthalpy of reaction for the measurements with a final isotherm at  $250\text{ }^\circ\text{C}$ ,  $270\text{ }^\circ\text{C}$  and  $285\text{ }^\circ\text{C}$  are reported in Figure S18, S19 and S20, respectively.

After DSC, a PXRD pattern of the samples was acquired for sample ramp  $250\text{ }^\circ\text{C}$  and  $285\text{ }^\circ\text{C}$  (Figure S21) and a Rietveld refinement was performed. The acquired cell parameters are close to those of sample S2, as reported in Table S11.

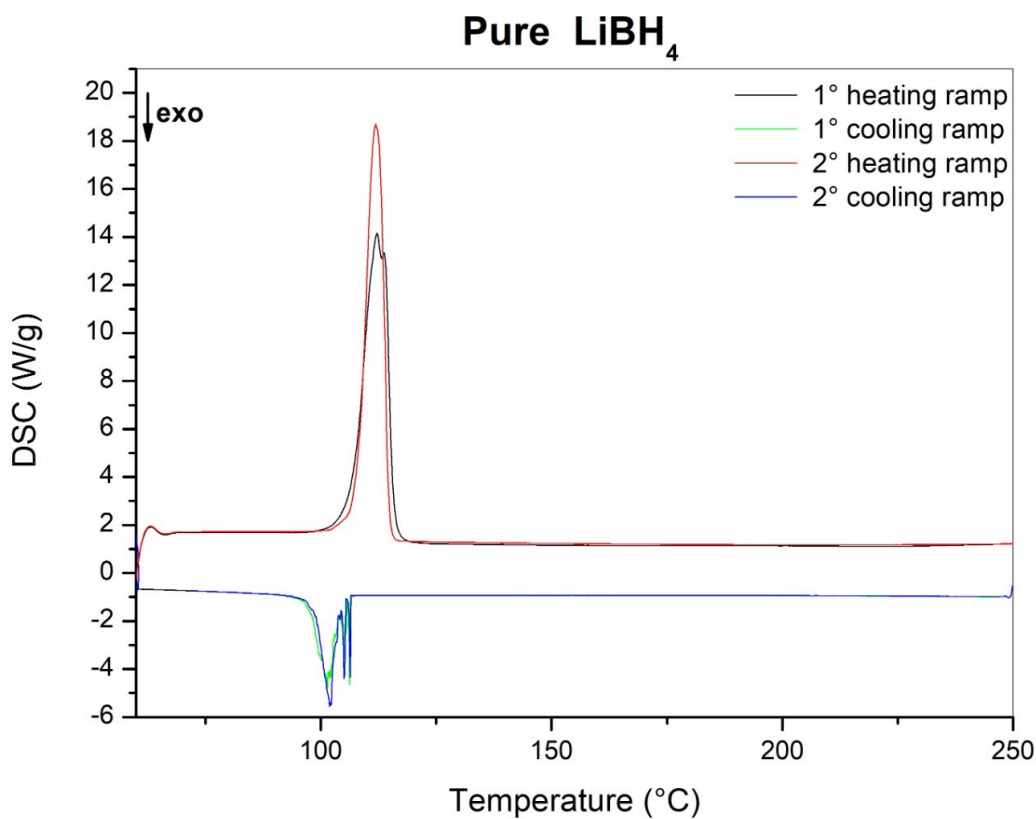
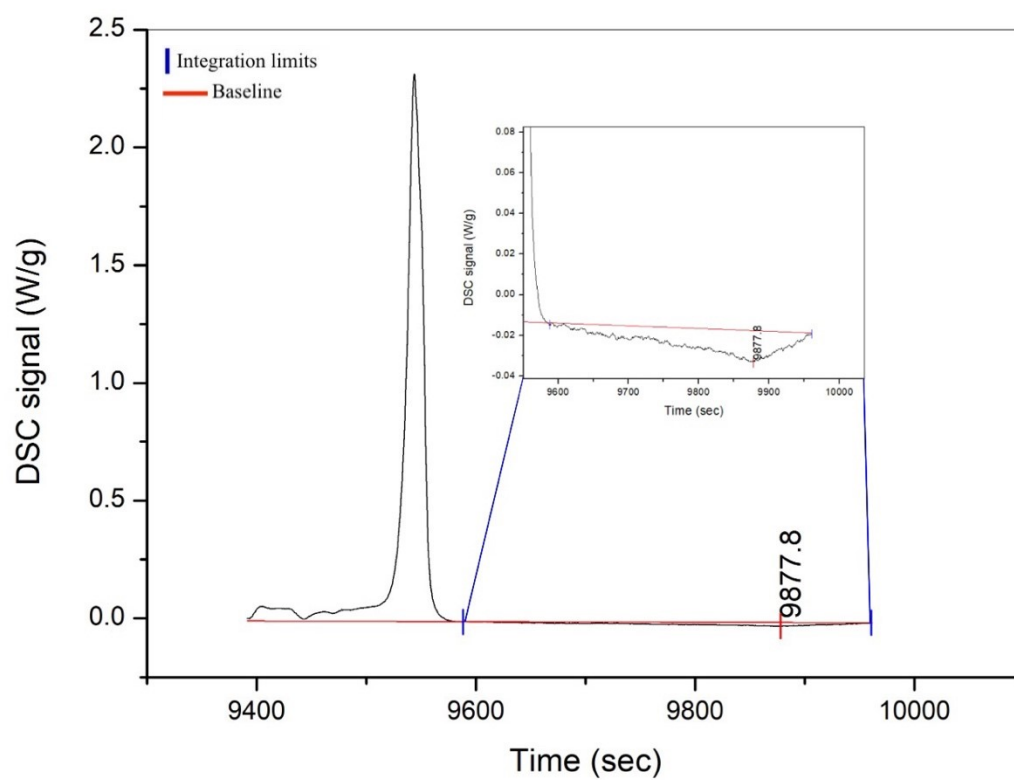
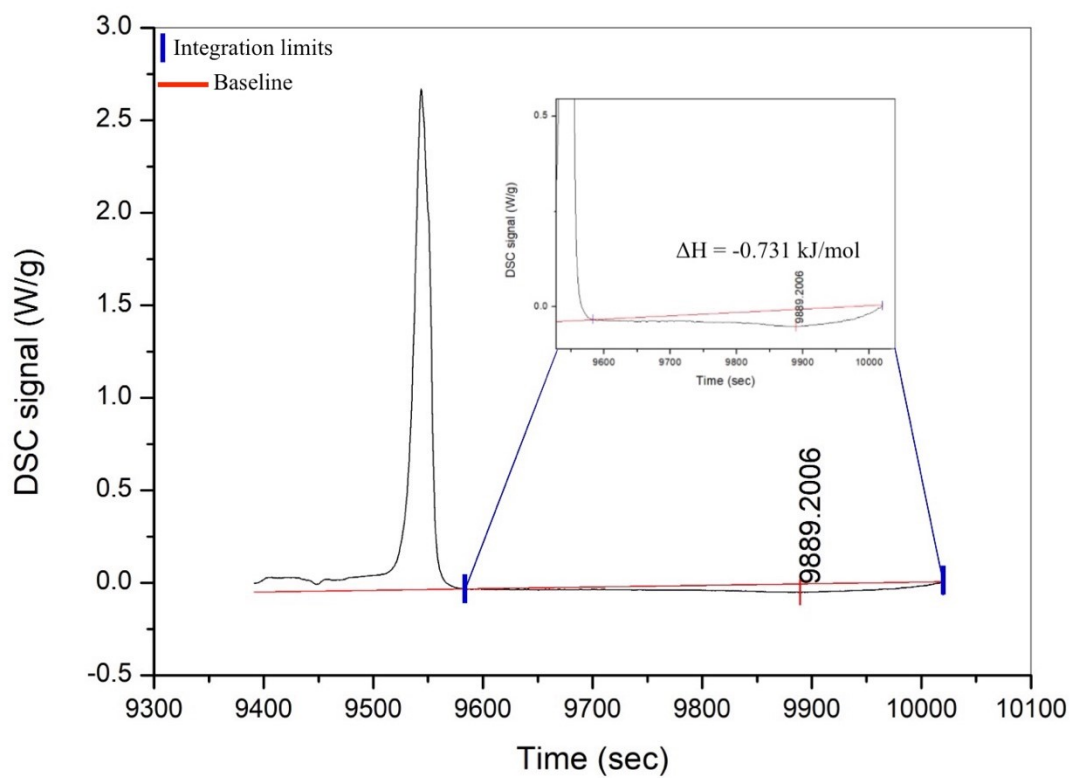


Figure S16 DSC trace of pure  $\text{LiBH}_4$



**Figure S17** Integration of the DSC signal correlated to the enthalpy of reaction for the formation of the hexagonal solid solution, after the subtraction of the second DSC trace from the first one, for the calorimetric analysis with the final isotherm at 250 °C.





**Figure S18** Integration of the DSC signal correlated to the enthalpy of reaction for the formation of the hexagonal solid solution, after the subtraction of the second DSC trace from the first one, for the calorimetric analysis with the final isotherm at 270 °C.

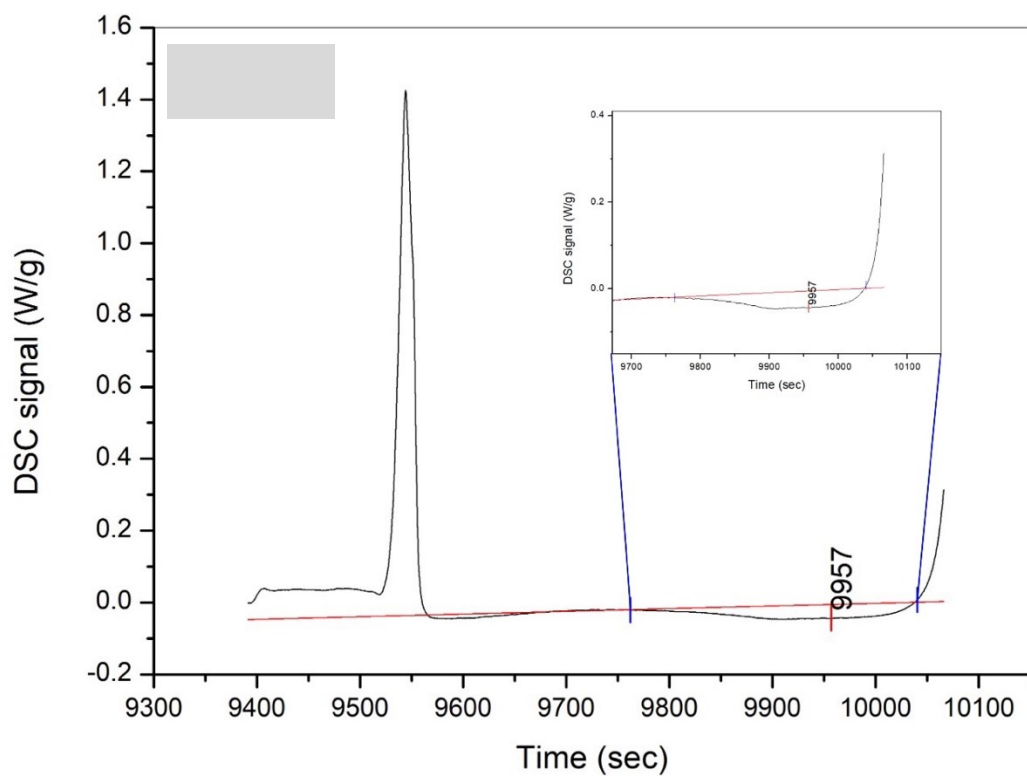


**Figure S19** Integration of the DSC signal correlated to the enthalpy of reaction for the formation of the hexagonal solid solution, after the subtraction of the second DSC trace from the first one, for the calorimetric analysis with the final isotherm at 285 °C.

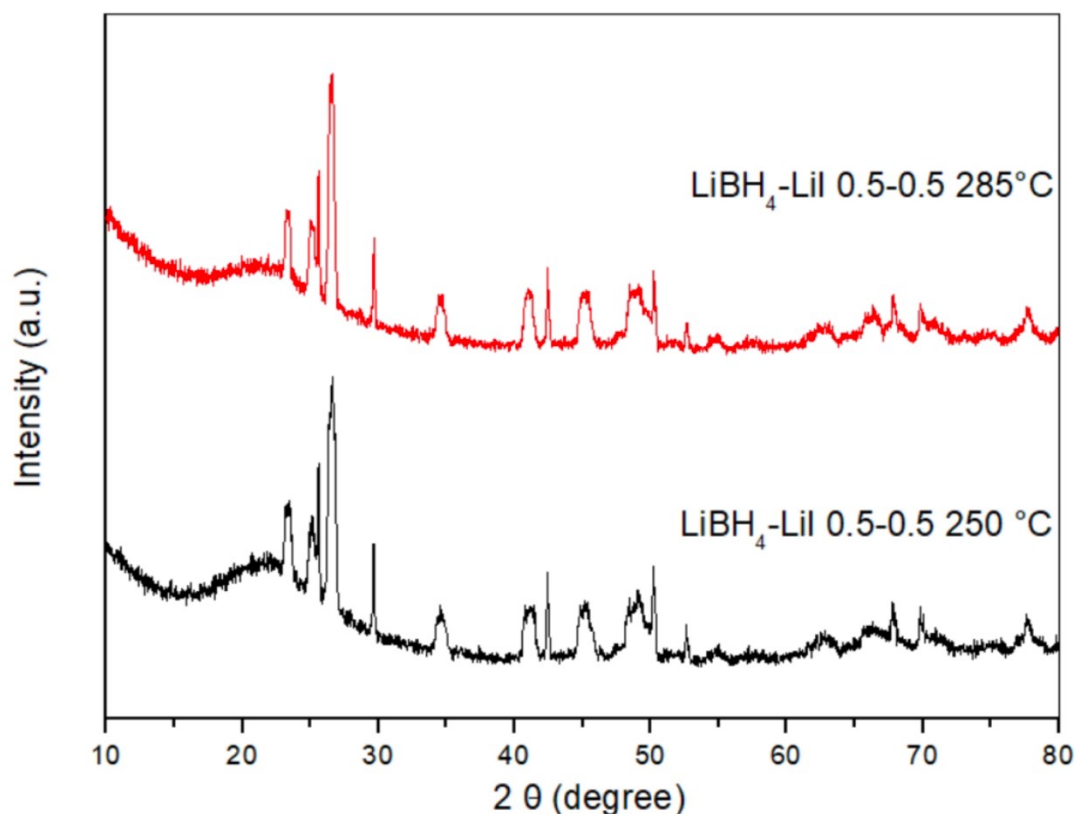


**Figure S20** PXRD traces of sample S9 after DSC measurements up to 250 °C (bottom) and 285 °C (top).

Sample	Cell parameter	
	a	c
S2	4.39	7.06
S9- 250°C isotherm	4.38	7.05
S9- 285°C isotherm	4.39	7.06

**Table S11** Cell parameters of sample S2 vs sample S9 after the DSC measurement for the enthalpy of mixing.

## References

1. Gulino Valerio. LiBH<sub>4</sub> as solid-state electrolyte for Li-ion Batteries: Modeling, Synthesis, Characterization and Application. Università degli Studi di Torino
2. Sveinbjörnsson D, Myrdal JSG, Blanchard D, Bentzen JJ, Hirata T, Mogensen MB, Norby P, Orimo SI, Vegge T. Effect of heat treatment on the lithium ion conduction of the LiBH<sub>4</sub>-LiI solid solution. *Journal of Physical Chemistry C*. 2013; <https://doi.org/10.1021/jp310050g>
3. Rude LH, Groppo E, Arnbjerg LM, Ravnsbæk DB, Malmkjær RA, Filinchuk Y, Baricco M, Besenbacher F, Jensen TR. Iodide substitution in lithium borohydride, LiBH<sub>4</sub>-LiI. *J Alloys Compd*. 2011; <https://doi.org/10.1016/J.JALLCOM.2011.05.031>